

Improving the Stability of an Integrated Power System With Stochastic Renewable Source Energies and Hybrid Power Flow Controller Using a Multi-Band Power System Stabilizer [†]

Seddiki Zahira ^{1,*}, Allaoui Tayeb ¹ and Smaili Atallah ¹

L2GI University of Tiaret; allaoui_tb@yahoo.fr (A.T.); Smaili_at@yahoo.fr (S.A.)

* Correspondence: zahira.seddiki@univ-tiaret.dz; Tel.: ((213) 0672916459)

[†] Presented at the 4th International Electronic Conference on Applied Sciences, 27 October–10 November 2023; Available online: <https://asec2023.sciforum.net/>.

Abstract: To ensure the stability of a multi-machine system with 4 generators and 11 nodes introduced by an hybrid power flow controllers (HPFC) and wind and solar sources, a multiband power system stabilizer (MB-PSS) is inserted in the system. In this work, the HPFC consists of two STATCOMs connected by a TCSC through a coupling transformer in a common DC link. The curves of the voltages at the nodes between the two zones and the curves of the active and reactive powers transmitted from one zone to the other are produced using the Matlab/simulink software.

Keywords: hybrid power flow controllers (HPFC); wind source; solar source; multiband power system stabilizer (MB-PSS); stability

1. Introduction

Ensuring the stability of the electrical system throughout its operation is becoming a major challenge, in accordance to the increase in electricity demand, the change in the topology of electrical networks and the insertion of renewable energies. The increased penetration of renewable energy sources, coupled with more sensitive voltage profiles, implies significant changes in the dynamics of system behavior. To damp the power oscillations, different kind of actuators are used such as power system stabilizers (PSSs) of generators, HVDC, flexible alternate current transmission systems (FACTSs) [1]. The hybrid power flow controllers (HPFC) introduced in the system controls the real power and regulates the voltage. It can also separately control the total reactive power exchanged with the transmitting and receiving ends of the line. Three configurations of HPFC are proposed by [2], proposed for the popular Western System Coordinated Council (WSCC) 3-machines 9-bus power system and investigated their effectiveness in enhancing the transient stability of the multi-machine system. Several realistic scenarios have been stimulated to demonstrate the potential benefits of the HPFC. The authors also tested different HPFC configurations on a Single-Machine Infinite Bus (SMIB) system and concluded that the HPFC is a better option for enhancing the stability of power systems [3]. Likewise, in [4], the performance of HPFC was assessed on two synchronous machines interconnected through transformers and transmission lines. The results demonstrated the capability of HPFC to control the power flow through the lines and improve the performance of the power system. In [5]. The authors used steady-state models of the HPFC to solve the power flow and optimal power flow (OPF) for the Ontario-Canada grid.

An HPFC controller is proposed in [6] for the Kundur 2-area 4-machines 12-bus system, evaluated under different control modes including PVV mode, PQQ mode, Impedance mode, and Voltage mode.

Citation: Zahira, S.; Tayeb, A.; Atallah, S. Improving the Stability of an Integrated Power System With Stochastic Renewable Source Energies and Hybrid Power Flow Controller Using a Multi-Band Power System Stabilizer. *2023*, *52*, x. <https://doi.org/10.3390/xxxxx>

Academic Editor(s):

Published: date



Copyright: © 2023 by the authors. Submitted for possible open access publication under the terms and conditions of the Creative Commons Attribution (CC BY) license (<https://creativecommons.org/licenses/by/4.0/>).

On the other hand, Power System Stabilizers (PSS), have been used for many years as an auxiliary controller to provide sufficient damping to the power system. Recent work on MB-PSS, has been applied in [7] in the Hydro-Québec power plant where it offered good performance at all frequencies. A combined control of STATCOM and MB-PSS is developed by [8] to improve power system stability and regulate the system voltage in Kundur's power system.

In this work, the HPFC consists of two shunt static compensators (STATCOM), connected by a thyristor controlled series compensator (TCSC) through a coupling transformer in a common DC link. This manuscript presents the efficiency of inserting the multiband power system stabilizer (MB-PSS) into a multi-machine system with 4 generators and 11 nodes, integrated by wind and solar sources, and controlled by a hybrid power flow controller (HPFC). The curves of the voltages at the nodes between the two zones and the curves of the active and reactive powers transmitted from one zone to the other are produced using the Matlab/simulink software. The results are useful, following sections throughout the paper: Section 2 presents a detailed description of the basic power system configuration with the Hybrid Power Flow Controller, following by section 3 reserved to study the stability of electrical system by Multi-Band Power System Stabilizer. In section 4, an overview is devoted to the insertion of renewable energy sources into the electricity network. The simulation results and discussion are presented in Section 5 and finally, section 6 summarizes the conclusions of the paper.

2. Basic Operation of the Hybrid Power Flow Controller HPFC

The HPFC is a combination of two-voltage source converters (VSC) connected in series and used to exchange the real power, and a controllable reactive power susceptance BM connected in shunt between the two VSCs as shown in Figure 1 below [9]

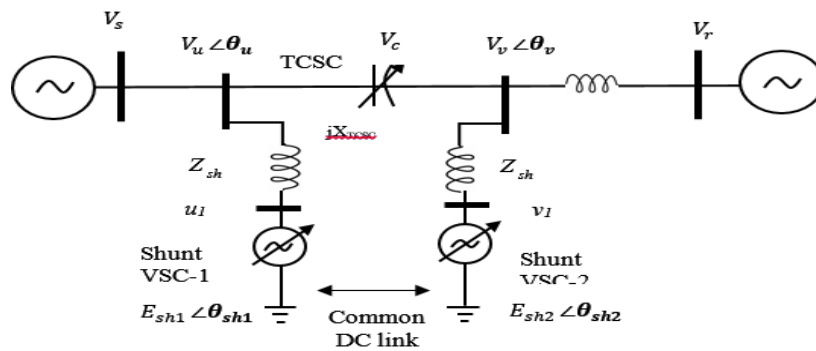


Figure 1. Typical Hybrid Power Flow Controller (HPFC).

The current flowing through the line is given in Equation 1.

$$I = (Vs - Vr - Vc) / X \tag{1}$$

Where:

$$Vs = |Vs| \angle \frac{\delta}{2}$$

$$Vr = |Vr| \angle \frac{\delta}{2}$$

$$Vc = |Vc| \angle \theta c$$

The actual impedance of the transmission line after installing the HPFC constituted of TCSC and STATCOMs, is the summation of initial impedance line and TCSC impedance as shown in Equation 2:

$$X = Xline + XTCS \tag{2}$$

3. Stability of Electrical System by Multi-Band Power System Stabilizer (MB-PSS)

Power System Stabilizer controllers are the most specific systems for improving the damping of low frequency oscillations in electrical networks [10], in line for their simplicity, ease of installation, their efficiency and reduced cost. They are present in almost every power system and present relatively high control efficiency [1]. The conventional PSS (CPSS) remains the most used PSS because of its simple structure and reliable in maintaining stability to small disturbances. The input signal is selected based on the effectiveness of various observable and controllable inputs signals for power oscillation damping. The input signal may include line current flow, line active power flow, line reactive power flow, and bus voltage [11].

The multi-band PSS is a particular conventional PSS designed to absorb all disturbances that occur in electrical networks. It is composed of three distinct bands dedicated to low, intermediate and high frequency oscillation modes. The input signal can be the power variation ΔP , the speed variation $\Delta\omega$ or the frequency variation Δf . Each band consists of a differential bandpass filter 'filter washout', an amplifier block and a limiter as indicated in Figure 2 below [12].

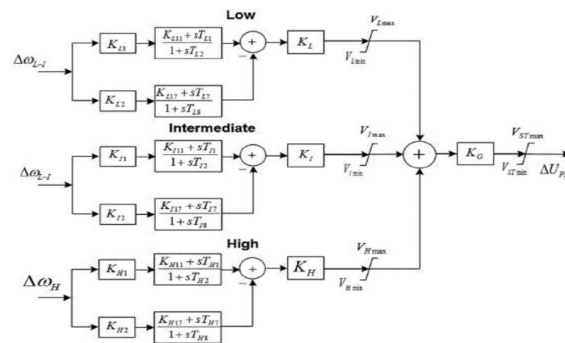


Figure 2. Typical Multi-Band PSS Configuration.

Each band is considered as a CPSS which can be described by the following transfer function:

$$\frac{V_{out}}{V_{in}} = K_{pss} \cdot \left(\frac{sT_w}{1 + sT_w} \right) \left(\frac{1 + sT_1}{1 + sT_2} \right) \left(\frac{1 + sT_3}{1 + sT_4} \right) \tag{3}$$

Where:

V_S Output of CPSS.

$\Delta\omega$ or ΔP Input of CPSS.

K_{pss} Gain of the conventional PSS Gain of the conventional PSS.

T_w Time constant of the first-order high-pass filter (sec).

T_1, T_2 Time constants of the first lead-lag transfer function (sec).

T_3, T_4 Time constants of the second lead-lag transfer function (sec).

4. Insertion of Renewable Energy

Considering the fluctuation of wind and sun, the analysis is based on real data from solar and wind sources during the winter season. The wind turbine is affected by winds of different speeds oscillating from 1.54 m/s to 4.63 m/s with a nominal power of 30 watts, while solar radiation varies from 60 watt/m² to a maximum value of 358 watt/m² as shown in the following data, as shown in Table 1 [13]:

Table 1. Values of wind speed and solar irradiation.

| Simulation Time (sec) | Solar radiation (Watt/m ²) | Wind speed (m/s) |
|-----------------------|--|------------------|
| 0 | 141 | 2.57 |
| 3 | 253 | 2.05 |
| 6 | 327 | 2.57 |
| 9 | 358 | 3.08 |
| 12 | 345 | 1.54 |
| 15 | 288 | 1.54 |
| 18 | 191 | 3.61 |
| 21 | 60 | 4.63 |

The Wind power can be based on Weibull probability distribution function $f(v)(v)$, with shape factor k and scale factor c . The probability of wind speed at specified time is given in Equation 4 [14,15].

$$f_{(v)}(v) = \left(\frac{k}{c}\right) \left(\frac{v}{c}\right)^{(k-1)} e^{-\left(\frac{v}{c}\right)^k}, \quad 0 < v < \infty \tag{4}$$

The power P extracted by a wind turbine, in Watts, is function of ρ the air density, A the area of wind turbine blade, v the wind speed and C_p the power coefficient. The distinguished speeds in the wind system are the cut-in speed v_{in} , the cut out speed v_0 and the rated speed of wind turbine system v_r , in m/s, as in Equation 5 [16].

$$\begin{cases} P = 0 & , \quad v < v_{in} \\ P = \frac{1}{2} \rho A v^3 C_p \left(\frac{v - v_{in}}{v_r - v_{in}}\right) & , \quad v_{in} \leq v \leq v_r \\ P = \frac{1}{2} \rho A v^3 C_p & , \quad v_r \leq v \leq v_{out} \\ P = 0 & , \quad v > v_{out} \end{cases} \tag{5}$$

The Weibull probability distribution function (wblpdf) is implemented in the Minitab program, giving scale = 3.0324 and shape = 2.9361 and is plotted against wind speeds in each time interval, Survival Function and Hazard Function, as in Figure 3.

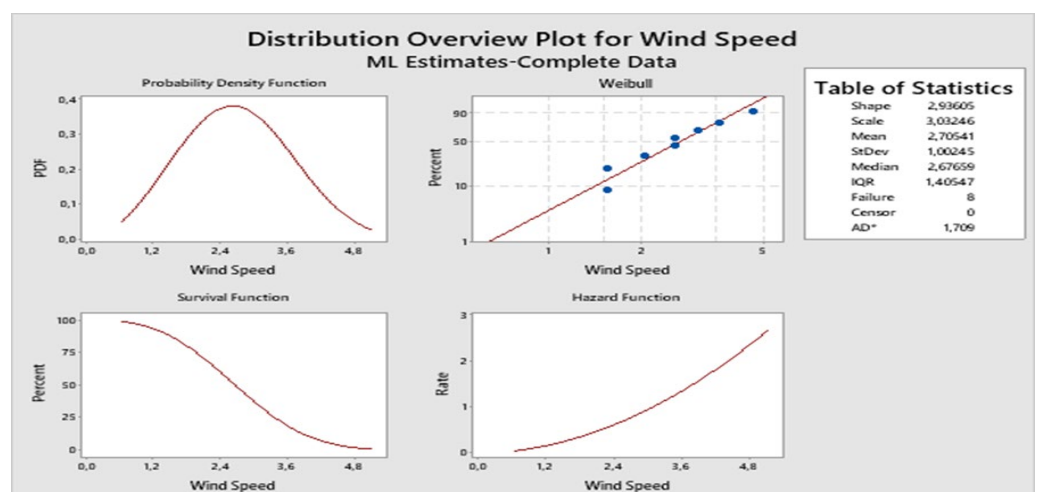


Figure 3. Distribution overview plot: Wind Speed.

In addition, the Weibull probability distribution function (wblpdf) is implemented in the Minitab program for solar irradiation, giving scale = 275,276 and shape = 2.7592, and is plotted in each time interval, Survival Function and Hazard Function, as in Figure 4.

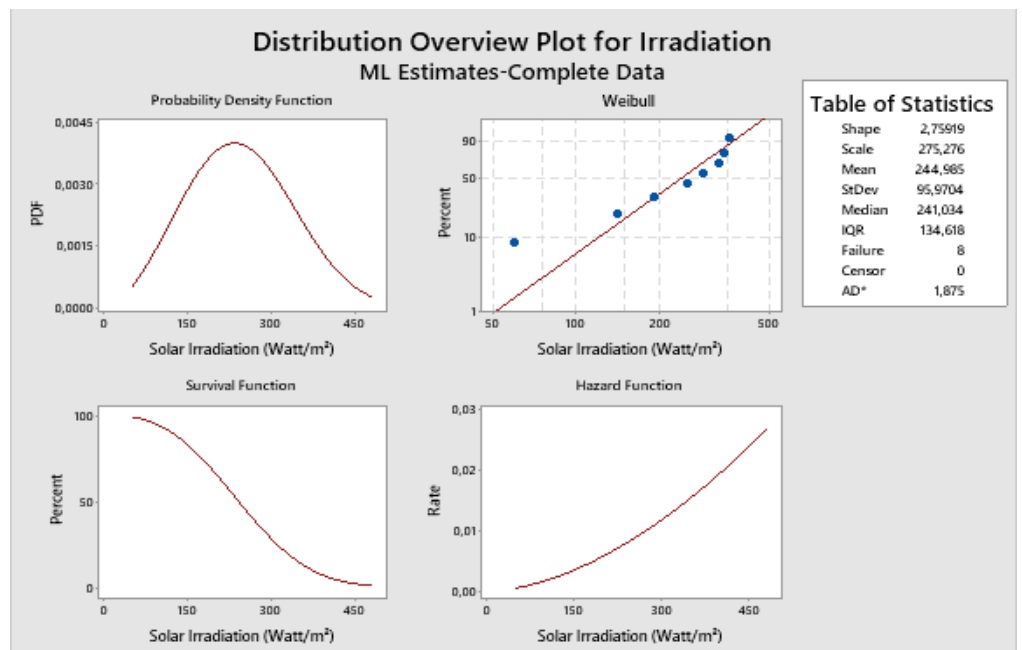


Figure 4. Distribution overview plot: Solar Irradiation.

5. Results Interpretation

The Kundur electrical network 04 generators_11 nodes (Figure 5) consists of two fully symmetrical zones linked together by two 230 kV lines 220 km long, where zone 1 exports 413 MW to zone 2. Each zone is equipped with two identical generators of 20kV/900MVA. The synchronous machines have identical parameters, with inertias $H = 6.5$ s in zone 1 and $H = 6.175$ s in zone 2. All generators produce approximately 700 MW each. Additional 187 Mvar capacitors are installed in each zone [17].

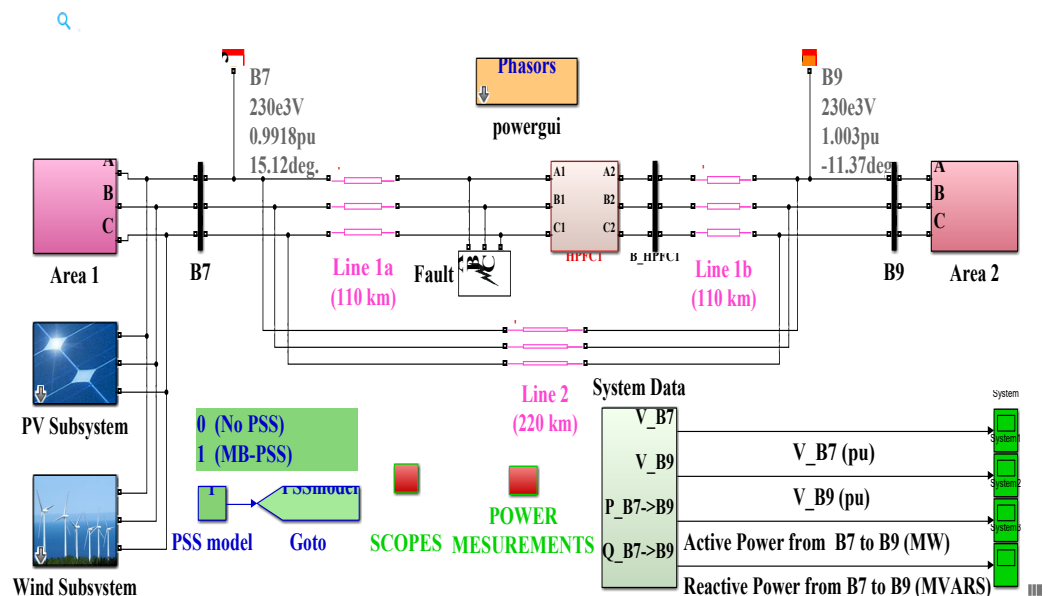


Figure 5. MATLAB/SIMULINK based model of Kundur electrical system equipped with wind and solar sources, MB-PSS and HPFC.

Initially, the active power and reactive power curves transmitted between zone 01 and zone 02, as well as the voltages retained at the level of each zone are schematized in Figures 6 below, without the presence of any source. Renewable or control mode.

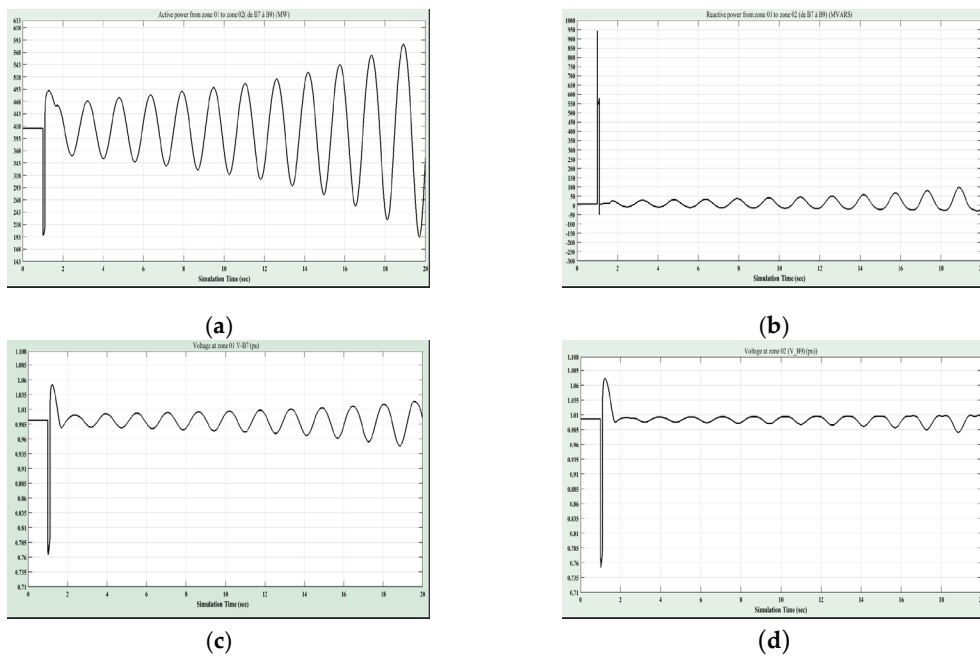


Figure 6. System without control and renewable sources (a) Active power from zone 01 to zone 02; (b) Active power from zone 01 to zone 02; (c) Voltage at zone 01; (d) Voltage at zone 02.

The system in presence of Renewable sources and is then subjected to Multi-Band PSS. The active power and the reactive power curves transmitted between zone 01 and zone 02, and the voltages retained at each zone are schematized in Figure 7 below.

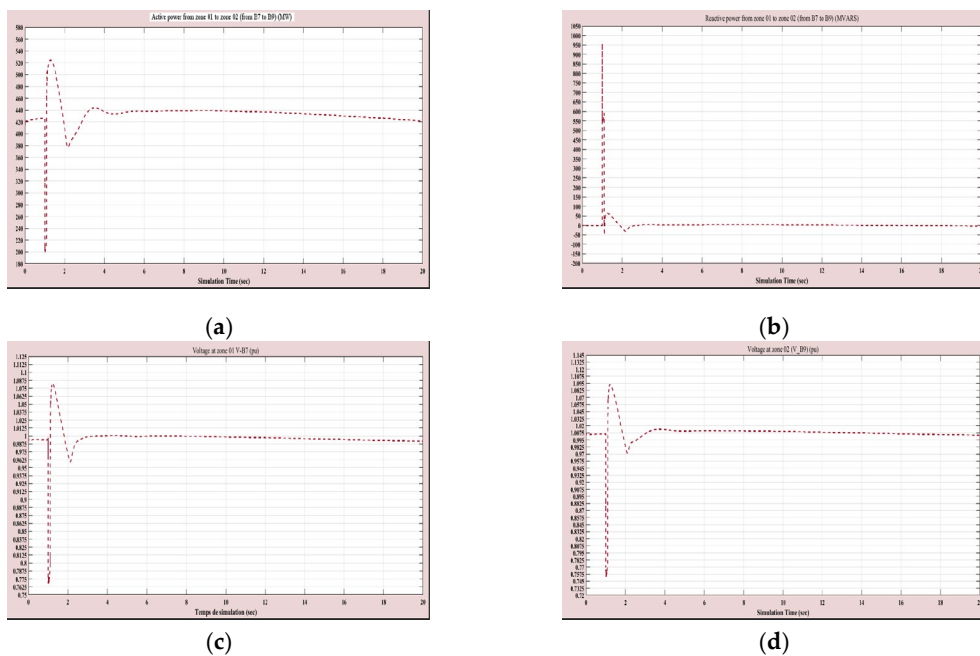


Figure 7. System with Renewable sources and MB-PSS: (a) Active power from zone 01 to zone 02; (b) Active power from zone 01 to zone 02; (c) Voltage at zone 01; (d) Voltage at zone 02.

Based on the obtained results from Figure 6 and Figure 7, and following the evaluation of the network parameters (transit power, voltage bus profile, etc.), it is perceived that the system is unstable during the simulation. To guarantee the system transient stability, the proposed combination of MB-PSS-HPFC presented in the paper is one of the solutions for this problem. By adding a Multi_Band PSS to each generator in the system, it is clearly observed that the negative effects of voltage regulators are removed and then

the damping of low-frequency oscillations is increased. Consequently, the system becomes stable.

Continuously, we proceeded to simulate the network under different fault values to determine the critical fault clearance time CFCT (Critical Fault Clearing Time). It is the time defined as being the maximum duration of the fault allowing the network to remain stable or to recover a new equilibrium state [18], as well as the time of loss of synchronism if applicable, as indicated in Figure 8.

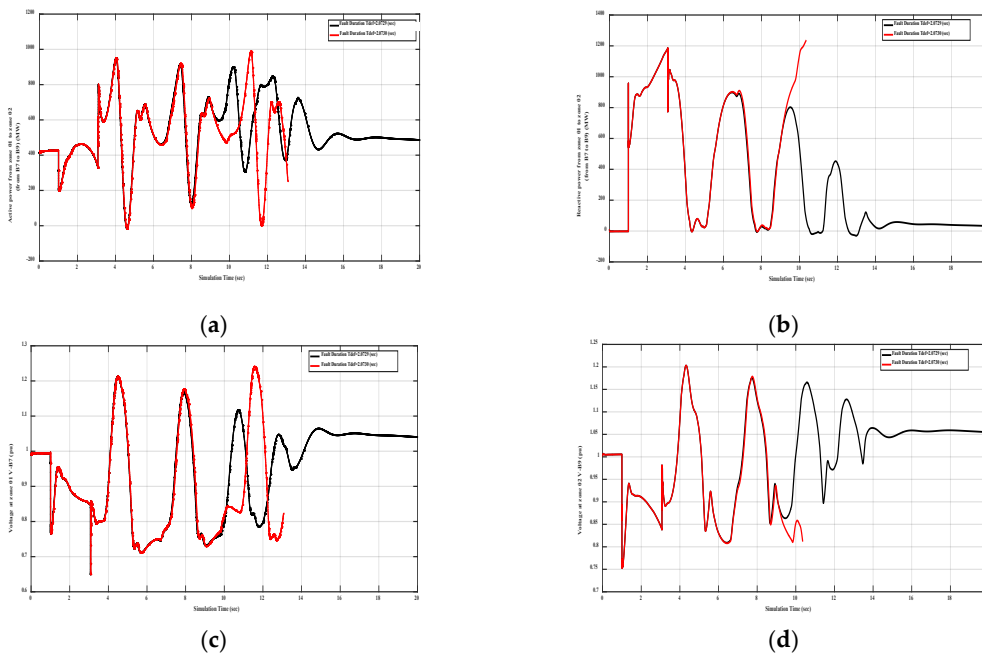


Figure 8. Critical Fault Clearing Time CFCT: (a) Active power from zone 01 to zone 02; (b) Active power from zone 01 to zone 02; (c) Voltage at zone 01; (d) Voltage at zone 02.

Finding the critical fault clearance time (CFCT) of the system is very necessary in transient stability. From Figure 9, it is seen that the loss of the stability is reached after 2,0729 seconds of simulation. The presence of the Multi-Band PSS delays.

6. Conclusion

The objectives of the study of electrical systems focused on the inter-zone area, is to detect and avoid stability problems linked to the operation of the network and, therefore, to secure the integration of renewable energies into the electrical network. The main objective is to control the operation of the entire system from measurements of power and transmission voltages across the network. Kundur 4 machine 11 bus system is the famous network used in the analysis and study of inter-area stability oscillations. The stability of in the presence of wind and solar power sources is tested in the presence of Multi-Band Power System Stabilizer (MB-PSS) and Hybrid Power Flow Controller (HPFC). The curves of active and reactive powers inter-zone and of the voltages at each zone are plotted using Matlab/Simulink software. The results confirm the reliability of PSS to prove the stability of the network. In another way, the critical fault clearance time (CFCT) of the system is determined, and confirms that the loss of stability is delayed and reached after 2,0729 seconds of simulation.

Author Contributions: This research article is prepared by Seddiki Zahira, Pr. Allaoui Tayeb and Pr. Smaili Atallah. The authors prepare, write, supervise and revise the original manuscript. They agree to the published version of the manuscript.

References

1. Karavas, C. S. G.; Plakas, K. A.; Krommydas, K. F.; Kurashvili, A. S.; Dikaiakos, C. N.; Papaioannou, G. P. A review of wide-area monitoring and damping control systems in Europe. *IEEE Madrid PowerTech* **2021**, 1-6.
2. Mathew, L and Chatterji, S. Transient Stability Analysis of Multi-Machine System Equipped with Hybrid Power Flow Controller. *International Journal of Computational Engineering and Management* **2012**, 15(4), pp. 1-10.
3. Mathew, L and S, Chatterji. Modeling and simulation of Hybrid Power Flow Controller implemented on SMIB system. *North American Power Symposium (NAPS) IEEE* **2014**, pp. 1-7.
4. Allali, K.; Azzag, E.B.; Kahoul, N. Modeling and Simulation of a Wind-diesel Hybrid Power System for Isolated Areas. *International Journal of Computer Applications* **2015**, 116(23), pp. 18-24. doi. 10.5120/20499-2409
5. Tamimi, B.; Canizares, C.; Battistelli, C. Hybrid power flow controller steady-state modeling, control, and practical application; *IEEE Transactions on Power Systems* **2016**, 32(2), pp. 1483-1492.
6. Murugan, A and Ramakrishnan, V. Modeling of HPFC Controller Using Multi-Machine Power System with Acting as Different Control Modes. *International Journal of Recent Technology and Engineering (IJRTE)* **2019**, pp. 120-124.
7. Grondin, R.; Kamwa, I.; Trudel, G.; Taborda, J.; Lenstroem, R.; Baumberger, H.; Gérin-Lajoie, L.; Gingras, J/P.; Racine, M. THE MULTI-BAND PSS, A FLEXIBLE TECHNOLOGY DESIGNED TO MEET OPENING MARKETS. *Cigré General, Paris, France* **2000**, pp. 39-201.
8. El-Sadek, M. Z.; Shabib, G.; Mobarak, Y.A.; El-Ahmar, M.H. COMBINED CONTROLS OF STATCOM DEVICE AND MULTI-BAND POWER SYSTEM STABILIZER (MB-PSS) IN POWER SYSTEM. *Journal of Engineering Science, Assiut University* **2009**, 37(1), pp. 115-124.
9. Anjali, A.B.; Mathew, L. Real Time Simulation of Hybrid Power Flow Controller. *International Journal of Grid and Distributed Computing* **2020**, 13(1), 388-399.
10. Fergane, M. Les Méthodes D'amélioration De La Stabilité Dynamique Dans Les Réseaux Electriques. Magister's Memory, University of FERHAT ABBAS, Sétif- Algeria, **2014**.
11. EL-Shimy, M.; Bekhet, M.; Metwali, F.; Bendary, A.; Mansour, W. M.; Mandour, M. A. FACTS-Based Stabilization of the Dynamic Stability of Weakly Interconnected Systems Considering Wind Power Integration. *Journal of Science and Technology*. **2017**, 4 (3), pp. 28-42.
12. Cherif, N.A.; ALLAOUI, T; Benacla, M. The Use of Multiband PSS to Improve Transient Stability of Multimachine Power System. *International Journal of Power Electronics and Drive Systems* **2013**, 3(3), 298-303.
13. <https://en.tutiempo.net/solar-radiation/toronto>.
14. Ranjit, R.; Jadhav, H.T. Optimal power flow solution of power system incorporating stochastic wind power using Gbest guided artificial bee colony algorithm. *International Journal of Electrical Power & Energy Systems Journal of Grid and Distributed Computing* **2015**, 64, 562-578.
15. Riaz, M.; Hanif, A.; Hussain, S.J.; Memon, M.I.; Ali, M.U.; Zafar, A. An Optimization-Based Strategy for Solving Optimal Power Flow Problems in a Power System Integrated with Stochastic Solar and Wind Power Energy. *Appl. Sci.* **2021**, 11, 6883.
16. BISWAS, P.P. Evolutionary algorithms for solving power system optimization problems. Doctoral thesis, Nanyang Technological University, Singapore, 2019.
17. Kundur, P. Power System Stability And Control, ch.12, sec. 8; McGraw-Hill, Inc: Toronto, Canada, 1994; pp. 813-814.
18. Bey, M. Impact d'une combinaison SMES IPFC sur le comportement d'un réseau électrique multi-machine, Doctoral thesis, Ibn Khaldoun University, Tiaret, Algeria, 2018.

Disclaimer/Publisher's Note: The statements, opinions and data contained in all publications are solely those of the individual author(s) and contributor(s) and not of MDPI and/or the editor(s). MDPI and/or the editor(s) disclaim responsibility for any injury to people or property resulting from any ideas, methods, instructions or products referred to in the content.